Available online at www.sciencedirect.com
ScienceDirect
Journal of Magnetic Resonance 184 (2007) 108–113
JMR Journal of Magnetic Resonance
www.elsevier.com/locate/jmr

Measuring fast hydrogen exchange rates by NMR spectroscopy

Fatiha Kateb [a], Philippe Pelupessy [a,*], Geoffrey Bodenhausen [a,b]

[a] Ecole Normale Supérieure, Département de Chimie, associé au CNRS, 24 rue Lhomond, 75231 Paris Cedex 05, France
[b] Ecole Polytechnique Fédérale de Lausanne, Laboratoire de Résonance Magnétique Biomoléculaire, Batochime, CH-1015 Lausanne, Switzerland

Received 31 July 2006; revised 12 September 2006
Available online 17 October 2006

Abstract

We introduce a method to measure hydrogen exchange rates based on the observation of the coherence of a neighboring spin S such as ^{15}N that has a scalar coupling J_{IS} to the exchanging proton I. The decay of S_x coherence under a Carr–Purcell–Meiboom–Gill (CPMG) multiple echo train is recorded in the presence and absence of proton decoupling. This method allows one to extract proton exchange rates up to $10^5\ s^{-1}$. We could extend the pH range for the study of the indole proton in tryptophan, allowing the determination of the exchange constants of the cationic, zwitterionic, and anionic forms of tryptophan.

Keywords: Hydrogen exchange; Proton transfer; Kinetic rates; Scalar relaxation

Nuclear magnetic resonance is a powerful tool to investigate hydrogen exchange [1]. Slow exchange rates can be measured by following in real time the replacement of hydrogen by deuterium [2]. Several methods have been developed to study fast and intermediate exchange, such as the analysis of the line-shape of exchanging protons [3], polarization transfer from the water resonance [4], decorrelation of longitudinal two-spin order [5] or measurements of translational diffusion coefficients [6]. Under favorable conditions, these methods allow one to measure rates up to a few thousand s^{-1}. It is also possible to investigate the line-shape of a coupled nucleus, which is affected by scalar relaxation of the second kind [7]. For small exchange rates, the spectra feature doublets separated by the scalar coupling constant J_{IS}, while in the limit of fast exchange the doublet collapses to a narrow singlet by a process called self-decoupling. Neglecting cross-correlated relaxation effects, the evolution of an initial in-phase coherence of a spin S such as ^{15}N coupled to an exchanging proton ^1H with spin I can be obtained by solving the Liouville equation

$$S_x(t) = S_x(0)\exp\{-vt - R(S_x)t\}\{\cosh(ut) + (v/u)\sinh(ut)\} \quad (1)$$

where $v = k/2$ and $u = (v^2 - \pi^2 J_{IS}^2)^{1/2}$, $k = k_{ex} + R(2S_xI_z) - R(S_x)$, $R(S_x)$ and $R(2S_xI_z)$ are the auto-relaxation rates of S_x and $2S_xI_z$, while k_{ex} is the exchange rate. In order to extract k, one can compare spectra recorded with and without proton decoupling [8]. However, in this case, long-range couplings $^nJ_{I'S}$ with $n > 1$ will also contribute to the undecoupled line-width, which can lead to erroneous measurements of fast exchange rates close to the self-decoupling limit. In order to eliminate these long-range couplings we propose to use a Carr–Purcell–Meiboom–Gill (CPMG) pulse-train [9] applied to the S spins and to detect the decay of the S_x coherence with and without proton decoupling. The π pulses in this echo train need not be closely spaced: typically, an interval $2\tau = 10$ ms between the pulses suffices to efficiently eliminate the effect of long-range scalar couplings $^nJ_{I'S} < 10$ Hz, while the larger short-range couplings retain their efficiency as a vehicle of scalar relaxation. Let A be a signal amplitude proportional to the in-phase coherence S_x remaining after a CPMG pulse-train *without* proton decoupling, and B a similar signal *with* decoupling. Fig. 1 shows the ratio A/B as a function of k for a scalar coupling $J_{IS} = 98.6$ Hz, a

* Corresponding author. Fax: +33 1 44 32 33 97.
E-mail address: philippe.pelupessy@ens.fr (P. Pelupessy).

1090-7807/$ - see front matter © 2006 Elsevier Inc. All rights reserved.
doi:10.1016/j.jmr.2006.09.022

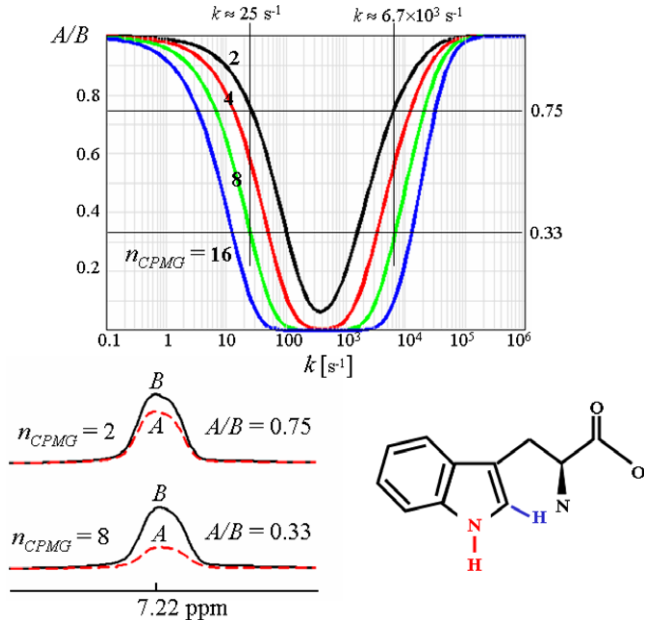

Fig. 1. (Top) Ratio A/B between the amplitude A of a ^{15}N coherence S_x of the n^{th}_{CPMG} echo of a Carr–Purcell–Meiboom–Gill (CPMG) pulse-train applied to ^{15}N nuclei *without* proton decoupling, and the amplitude B after a similar echo pulse-train *with* proton decoupling, as a function of the rate k defined in Eq. (1). The ^{15}N spin S is coupled to the exchanging proton I with a scalar coupling constant J_{IS}. The different curves correspond to different numbers n_{CPMG} of π pulses. The spacing 2τ between the π pulses was 10.6 ms, the amplitude of the RF field applied to the protons was $\nu_1 = 6$ kHz and $J_{IS} = 98.6$ Hz. The parameters of these simulations, calculated as explained in the Appendix A, correspond to the experimental conditions. The curves must be recalculated for different parameters. (Bottom right) In tryptophan, the polarization is transferred from the proton indicated in blue via its attached carbon-13 to the indole nitrogen-15. After a CPMG pulse train applied to ^{15}N in absence or presence of proton decoupling, the nitrogen coherence S_x is transferred back and detected on the proton of origin. (Bottom left) Experimental proton signals with amplitudes proportional to the indole nitrogen coherence S_x of tryptophan at pH 10.1 and 300 K, for $n_{CPMG} = 2$ and 8. The ratio A/B was 0.75 and 0.33 for $n_{CPMG} = 2$ and 8, respectively. This corresponds to a rate k of 6.7×10^3 s^{-1}. Note that a rate $k = 25$ s^{-1} would lead to the same ratio A/B.

radio-frequency (RF) field with an amplitude $\nu_1 = 6$ kHz, and $2\tau = 10.6$ ms for different numbers n_{CPMG} of π pulses.

The longer the pulse-train, the more time there will be for scalar relaxation to occur and hence the lower the ratio A/B will be. The measurement of exchange rates will be most precise for a number n_{CPMG} corresponding to the steepest curve at that rate. Our method is particularly advantageous for measurements of high exchange rates where $k \approx k_{ex}$. However, one has to realize that there is always a small contribution to k due to the longitudinal relaxation of the proton. An experiment with $n_{CPMG} = 2$ (hence with a total relaxation delay of $4\tau = 21.2$ ms) suffices to detect exchange rates up to 20×10^3 s^{-1}, while for a CPMG train with $n_{CPMG} = 16$ pulses (corresponding to a total relaxation delay of $32\tau = 169.6$ ms), exchange rates as large as 10^5 s^{-1} can be detected, with $A/B \approx 0.98$. This result may appear surprising, considering the fact that the RF amplitudes are far smaller than the exchange rates.

In order to test the methodology, we have studied the exchange rate of the indole proton of tryptophan in water as a function of pH and temperature. In previous studies [5,10] the highest exchange rates that could be detected were about $k_{ex} \approx 100$ s^{-1}. We transferred polarization from a neighboring proton via its attached carbon-13 ($^{13}C_2$) to the indole nitrogen-15 (see Fig. 2). The nitrogen coherence was allowed to decay partly under a CPMG pulse train without (signal intensity A) and with (signal B) proton decoupling. The remaining in-phase coherence S_x was transferred back to the proton of origin. In addition to nitrogen-15, carbon-13 labeling is necessary for this sequence. However, with cryogenically cooled probes direct detection of the nitrogen coherence is viable even at millimolar concentrations [11]. In Fig. 1 (bottom left), an example of the results at 300 K for pH 10.1 is shown for CPMG trains with $n_{CPMG} = 2$ and 8.

For a given ratio A/B two values of k are possible (see Fig. 1.) The line-shape of the S spin spectrum in principle allows one to resolve this ambiguity. For slow exchange rates, a doublet will be observed, while for fast rates the spectrum will consist of a singlet. For the intermediate exchange regime (i.e., when the ratio A/B is close to its minimum), however, it is not so easy to distinguish between the two solutions. An easy way to obtain the exchange rate unambiguously is to diminish the intervals 2τ between the π-pulses in the CPMG pulse train. In Fig. 3 (top), the curve for $n_{CPMG} = 2$ and $2\tau = 10.6$ ms of Fig. 1 is plotted again together with a calculation for $n_{CPMG} = 4$ and $2\tau = 5.3$ ms. The total relaxation time is the same. The minimum is shifted to the right for the latter curve. On the bottom of Fig. 3, experimental results are shown for pH 8.3 at 300 K. For $2\tau = 10.6$ ms and $n_{CPMG} = 2$, the ratio $A/B = 0.11$ is compatible either with $k = 213$ or 702 s^{-1}, while for $2\tau = 5.3$ ms and $n_{CPMG} = 4$, the ratio $A/B = 0.45$ agrees with $k = 214$ or 2050 s^{-1}. Only the lower value $k \approx 213$ s^{-1} is consistent with both experiments. A chemical exchange contribution R_{ex} to the nitrogen line-width due to fluctuations of the isotropic shift would equally affect the signal intensities in both experiments; hence the ratio A/B would not be affected. In order to minimize the contribution of R_{ex} to the decay of S_x, one may reduce the pulse interval 2τ. However, as can be seen in Fig. 3, the ratio A/B will be less sensitive to scalar relaxation in this case.

The CPMG pulse train diminishes effects of scalar relaxation due to remote protons I'. We found an empirical relationship $A/B = \{1 - 6.54 n_{CPMG} J_{I'S}{}^2 \tau^3 R_1(I')\}$ for the longitudinal relaxation rate of the remote proton $R_1(I') < 100$ s^{-1}. For $J_{I'S} = 5$ Hz, $\tau = 5.3$ ms, $n_{CPMG} = 16$ and $R_1(I') = 2$ s^{-1}, we obtain $A/B = 0.9992$. Thus the effect of remote protons can be safely neglected.

In Fig. 4, the theoretical and experimental ratio A/B is plotted as a function of the RF amplitude ν_1, for $k = 213$ s^{-1} ($2\tau = 10.6$ ms and $n_{CPMG} = 2$). For this exchange rate, the RF amplitude can be diminished to 1 kHz without affecting the ratio A/B significantly. For lower RF amplitudes, the ratio $|A/B|$ increases dramatically,

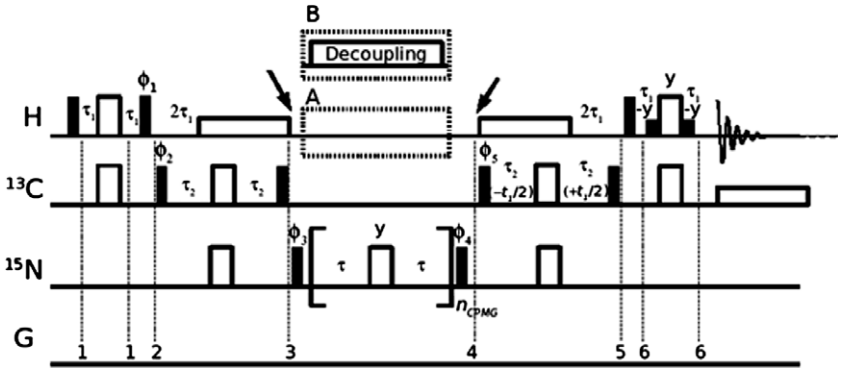

Fig. 2. Pulse sequence used for the measurement of the indole proton exchange rate k_{ex}. The polarization is transferred from the neighboring proton via the carbon-13 to the nitrogen-15. The coherence at the beginning of the CPMG period is thus $2N_yC_z$. Note that this coherence might be affected by longitudinal cross-correlated relaxation between the CSA of the carbon and the carbon-proton dipole-dipole interaction. However, for the relaxation delays considered, the effects of this rate are negligible in tryptophan. Narrow filled and wide open rectangles represent $\pi/2$ and π pulses, wide open bars depict decoupling sequences, the small filled rectangles show selective $\pi/2$ pulses on the water resonance. All phases are along the x-axis unless indicated otherwise. The frequency of the proton carrier is moved from the water resonance to the resonance of the indole proton just before the CPMG period (left arrow) and back thereafter (right arrow). In experiment A no proton decoupling is applied during the CPMG period while in experiment B a continuous wave RF field or a WALTZ-16 decoupling sequence is employed. The phase cycling was $\phi_1 = 16(y), 16(-y)$; $\phi_2 = x, -x$; $\phi_3 = 2(x), 2(-x)$; $\phi_4 = 4(x), 4(-x)$; $\phi_5 = 8(x), 8(-x)$ and the receiver phase was $x, -x, -x, x, 2(-x, x, x, -x), x, -x, -x, x, -x, x, x, -x, 2(x, -x,-x,x), -x, x, x, -x$. The delays for coherence transfer are $\tau_1 = 1/(4^1J_{CH})$ (1.56 ms) and $\tau_2 = 1/(4^1J_{CN})$ (16 ms). The sequence can easily be converted into a two-dimensional experiment by introducing a constant-time evolution period (in parentheses) for carbon-13, while incrementing ϕ_5 for States-TPPI quadrature detection. If one includes a nitrogen-15 evolution period, one should take care to decouple the protons continuously.

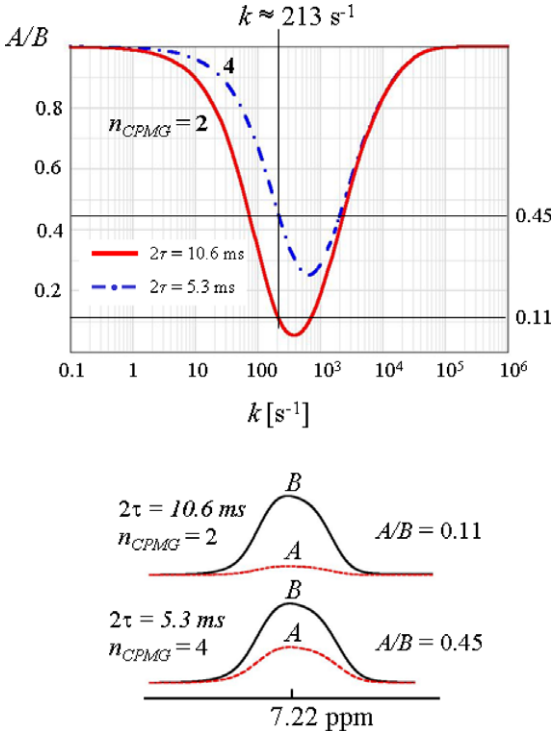

Fig. 3. Effect of changing the delay 2τ between the π pulses in the CPMG pulse train. (top) The red bold line corresponds to the calculated curve of Fig. 1 with $2\tau = 10.6$ ms and $n_{CPMG} = 2$, while the blue dashed curve is for $2\tau = 5.3$ ms and $n_{CPMG} = 4$, the other parameters being the same as in Fig. 1. (Bottom) Experiments performed on tryptophan at pH = 8.3 and $T = 300$ K using the pulse sequence of Fig. 2. The measured ratios $A/B = 0.45$ and 0.11 cross the two theoretical curves at four intersections, but only the two crossings on the left are in agreement with a single rate $k \approx 213\ s^{-1}$. (For interpretation of the references to color in this figure legend, the reader is referred to the web version of this paper.)

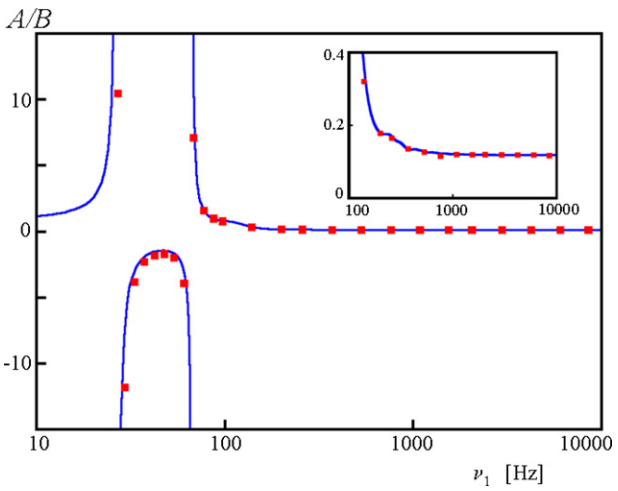

Fig. 4. The ratio A/B is plotted as a function of the radio-frequency (RF) amplitude $\nu_1 = \gamma B_1/(2\pi)$ for a rate $k = 213\ s^{-1}$, $2\tau = 10.6$ ms and $n_{CPMG} = 2$. The blue line corresponds to the theoretical curve, while the red squares represent the experimental values. The experiments were performed on tryptophan at pH = 8.3 and $T = 300$ K using the pulse sequence of Fig. 2. The insert shows and expansion for $0 < A/B < 0.4$. (For interpretation of the references to color in this figure legend, the reader is referred to the web version of this paper.)

since the signal intensity B becomes smaller, rendering the experiment less sensitive. Moreover, the calibration of the RF amplitude becomes critical.

The ratio A/B depends on the offset of the exchanging proton. In Fig. 5, the theoretical and experimental offset profile of the ratio A/B is plotted for $k = 213\ s^{-1}$ ($2\tau = 10.6$ ms, $n_{CPMG} = 2$ and $\nu_1 = 6$ kHz). It is clear that one can extract the exchange rate if the offset is known.

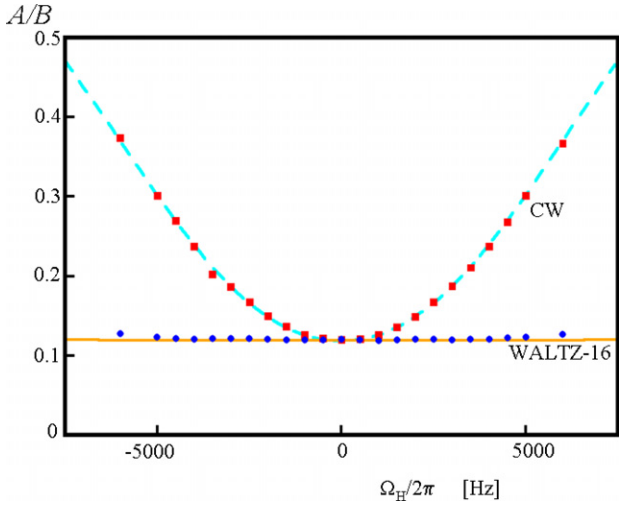

Fig. 5. Experimental and theoretical profiles of the ratio A/B (for an exchange rate 213 s^{-1}, $2\tau = 10.6$ ms, $n_{CPMG} = 2$ and $\nu_1 = 6$ kHz) as a function of the proton offset Ω_H with respect to the carrier frequency. The dashed blue and solid orange lines correspond to calculations using CW and WALTZ-16 decoupling, respectively. The red squares and blue circles are the experimental values of the ratio A/B for continuous wave and WALTZ-16 decoupling, respectively. The experiments were performed on tryptophan at pH = 8.3 and $T = 300$ K using the pulse sequence of Fig. 2. (For interpretation of the references to color in this figure legend, the reader is referred to the web version of this paper.)

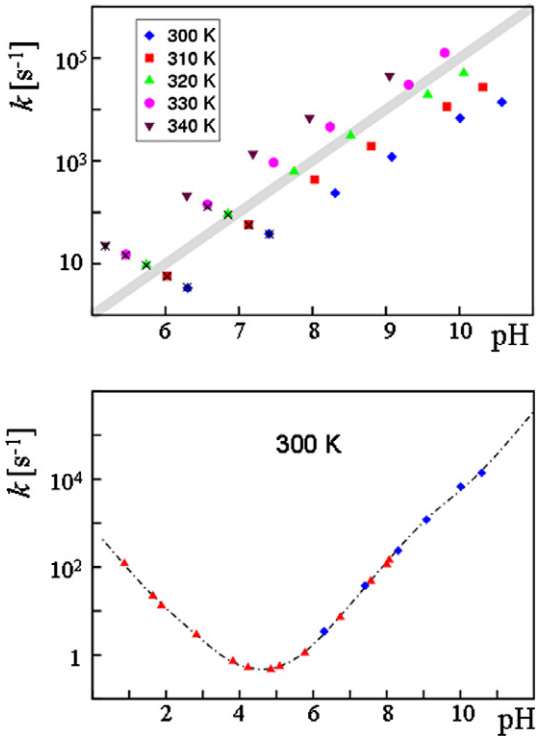

Fig. 6. (Top) Rates k of the indole proton in a 20 mM solution of ^{13}C and ^{15}N enriched tryptophan in H_2O at different temperatures as a function of pH. The rates have been determined by measuring the ratio A/B, after an echo train applied to the nitrogen nucleus S with $2\tau = 10.6$ ms, $n_{CPMG} = 2$, 4, 8 and 16 π pulses (for the details see Fig. 1). The upper limit of detection of the exchange rate is about 10^5 s^{-1}. Small exchange rates have also been measured by the method of Skrynnikov and Ernst [5] (denoted by ×). (Bottom) Measurements of the exchange rate at 300 K (blue diamonds), complemented at low pH by the measurements of decay rates of two-spin order $2N_zH_z^N$ by Skrynnikov and Ernst [5] (red triangles). The dashed line is a result of a fit using Eqs. (3) and (4) as described in the text. (For interpretation of the references to color in this figure legend, the reader is referred to the web version of this paper.)

If this is not the case, one can apply a broadband decoupling sequence. The offset profile of the same experiment using a WALTZ-16 decoupling sequence [12] instead of continuous-wave RF field is also plotted in Fig. 5. With WALTZ-16 decoupling, the ratio A/B is hardly affected up to offsets of 5 kHz.

In Fig. 6 (top), the extracted rates k are shown for different pH and temperatures. When possible we have also measured the relaxation rate of the $2N_zH_z^N$ two-spin order [5]. For low rates ($k < 100$ s^{-1}) this experiment is more sensitive and easier to perform. As explained in the Appendix, we have taken into account the presence of 6% HDO in our sample. This leads to a correction of at most 0.012 in the ratio A/B of Fig. 1. Note that the errors that occur when the small fraction of deuterium in the solvent is not taken into account lie within the size of the symbols of Fig. 6. The errors in the experimental ratios A/B were about 0.5% leading to errors in k which varied from 1 to 3%. Only for the measurement of the highest $k(T = 330$ K and pH = 9.8) did the experimental error exceed 3% ($k = 132 \times 10^3 \pm 24 \times 10^3$ s^{-1}).

In grey, a line with a slope of one is drawn in Fig. 6 to guide the eye. At high pH one expects a linear asymptote with a slope of 1 in this semi-logarithmic plot if one assumes a simple dependence of the exchange rates,

$$k_{ex} = k_H 10^{-pH} + k_{OH} K_W 10^{pH} \quad (2)$$

where k_H and k_{OH} are acid- and base-catalyzed exchange rate constants, and K_W is the auto-ionization constant of water ($K_W = 10^{-13.936}$ at 300 K). This is clearly not the case. In previous studies, deviations from Eq. (2) have already been noticed around pH 3. This was attributed to the deprotonation of the carboxyl group. In fact, there is an equilibrium between the cationic ($^+H_3NCHRCOOH$), zwitterionic ($^+H_3NCHRCOO^-$), and anionic ($H_2NCHRCOO^-$) forms of tryptophan. Each form may have its own exchange rate constants. The exchange rate is thus given by:

$$k_{ex} = k_{H_c} f_c 10^{-pH} + k_{OH_c} K_W f_c 10^{pH} + k_{H_z} f_z 10^{-pH} + k_{OH_z} K_W f_z 10^{pH} + k_{H_a} f_a 10^{-pH} + k_{OH_a} K_W f_a 10^{pH} \quad (3)$$

where the indices c, z, and a stand for the cationic, zwitterionic, and anionic forms and f for the fraction of each form, i.e.,

$$f_c = (1 + 10^{pH-pK_{a1}} + 10^{2pH-pK_{a1}-pK_{a2}})^{-1},$$
$$f_z = (1 + 10^{-pH+pK_{a1}} + 10^{pH-pK_{a2}})^{-1}, \quad (4)$$
$$f_a = (1 + 10^{-pH+pK_{a2}} + 10^{-2pH+pK_{a1}+pK_{a2}})^{-1},$$

where $pK_{a1} = 2.46$ refers to the carboxyl group, while $pK_{a2} = 9.41$ is associated with the amine group. At conditions where f_c is not negligible (low pH), the first term in Eq. (3) eclipses the second one. In a similar manner, the sixth term dominates the fifth term at high pH. Thus, only four of the six constants can be determined. The data at 300 K, complemented with the measurements of the decorrelation of two spin coherence $2N_zH_z$ by Skrynnikov and Ernst [5] at low pH, have been fitted to:

$$k = k_{ex} + C \tag{5}$$

For the experiment that measures the decorrelation of the two spin coherence, $C = R(2N_zH_z)$, i.e., the auto-relaxation rate of the zz order, while for the new experiment that quantifies the scalar relaxation, we have $C = R(2S_xI_z) - R(S_x)$. For the fit we have assumed these constants to be equal in both experiments, since for values of k_{ex} where the difference between the constants might be significant, only the decay of the zz order is measured. Specifically, at a pH around 5, the exchange rate k_{ex} is so low that one cannot neglect the contribution of $R(2N_zH_z)$. In Fig. 6 (bottom), the results of the fit are shown: $C = 0.37 \pm 0.01\ s^{-1}$, $\log(k_{H_c}/k_0) = 2.90 \pm 0.03$, $\log(k_{H_z}/k_0) = 3.31 \pm 0.03$, $\log(k_{OH_z}/k_0) = 8.06 \pm 0.01$, and $\log(k_{OH_a}/k_0) = 7.48 \pm 0.03$, where $k_0 = 1\ s^{-1}$. Protonation of the amine leads to an enhanced OH-catalyzed exchange, while the protonation of the carboxyl group reduces the H-catalyzed exchange. This is in agreement with the results of Molday et al. [13], who investigated the influence of neighboring side chains and adjacent peptide groups on amine exchange rates. An additional positive charge leads to a withdrawal of electrons from the indole position, thus increasing its acidity.

In conclusion, we have introduced a method to measure hydrogen exchange rates based on the comparison of the decay of the coherence of a coupling partner subjected to a CPMG pulse train with and without proton decoupling. This method allowed us to extract exchange rates up to $10^5\ s^{-1}$ for the indole proton in tryptophan.

Acknowledgments

We thank the CNRS and the ANR of France for financial support.

Appendix. Effect of deuterium in the solvent

The evolution of the density matrix ρ during the CPMG sequence is given by

$$\rho(t) = \{\exp(-L\tau)R_N \exp(-L\tau)\}^n \rho(0) \tag{A.1}$$

where L is the Liouvillian and R_N is the operator representing a π_y pulse applied to ^{15}N with $n = n_{CPMG}$. If there are no deuterons in the solvent, and if the RF carrier is on-resonance with respect to the ^{15}N chemical shift, a basis of four operators $\{N_y, 2N_xH_z, 2N_xH_x, 2N_xH_y\}$ suffices to describe the system. In this case the operators L and R_N are given by:

$$L = \begin{pmatrix} 0 & -\pi J_{NH} & 0 & 0 \\ \pi J_{NH} & k & 0 & -\omega_1 \\ 0 & 0 & k & \Omega_H \\ 0 & \omega_1 & -\Omega_H & k \end{pmatrix}$$

$$R_N = \begin{pmatrix} 1 & 0 & 0 & 0 \\ 0 & -1 & 0 & 0 \\ 0 & 0 & -1 & 0 \\ 0 & 0 & 0 & -1 \end{pmatrix} \tag{A.2}$$

where ω_1 is the amplitude of the RF field applied to the protons while Ω_H is the offset of the exchanging proton from the carrier. Transverse relaxation of ^{15}N does not affect the ratio A/B. To obtain this ratio, the evolution of the density operator needs to be calculated twice according to Eq. (A.1), once with $\omega_1^{(A)} = 0$, and once with $\omega_1^{(B)}$ set to the RF amplitude used in the experiments. If there is deuterium in the solvent, the normalized basis of the density operator must be extended to $\{(1/\sqrt{3})N_y^H E^H E^D, (2/\sqrt{3})N_x^H H_z E^D, (2/\sqrt{3})\ N_x^H H_x E^D, (2/\sqrt{3})N_x^H H_y E^D, (1/\sqrt{3})\ N_y^D E^H E^D, (1/\sqrt{6})\ N_y^D E^H (3D_z^2 - 2E^D), (1/\sqrt{2})N_y^D E^H D_z\}$. The symbols N^H and N^D refer to nitrogen nuclei coupled to exchanging protons or deuterium nuclei; E^H and E^D represent unity operators in their respective subspaces. With the usual product operator conventions, $N_y^H E^H E^D$ is simply denoted by N_y^H. Note that there are no transverse terms of deuterium angular momentum in the absence of an RF field applied to this nucleus. In this basis the Liouvillian is:

$$L = \begin{pmatrix} fk & -\pi J_{NH} & 0 & 0 & -(1-f)k & 0 & 0 \\ \pi J_{NH} & k & 0 & -\omega_1 & 0 & 0 & 0 \\ 0 & 0 & k & \Omega_H & 0 & 0 & 0 \\ 0 & \omega_1 & -\Omega_H & k & 0 & 0 & 0 \\ -fk & 0 & 0 & 0 & (1-f)k & 0 & (4/\sqrt{6})\pi J_{ND} \\ 0 & 0 & 0 & 0 & 0 & k & (2/\sqrt{3})\pi J_{ND} \\ 0 & 0 & 0 & 0 & -(4/\sqrt{6})\pi J_{ND} & -(2/\sqrt{3})\pi J_{ND} & k \end{pmatrix} \tag{A.3}$$

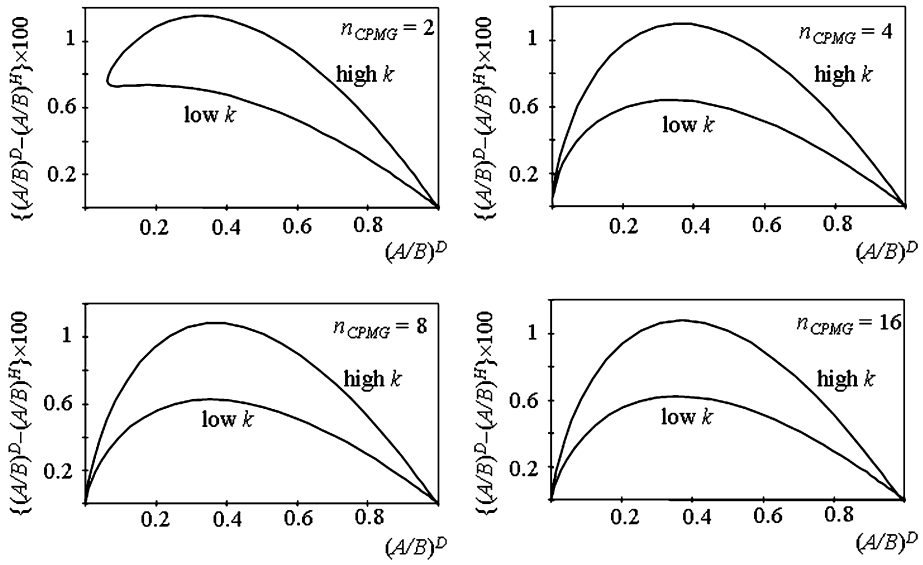

Fig. A1. Deviations caused by partial deuteration of the solvent. $(A/B)^{D}$ is the ratio in the presence of 3% deuterated water. After subtracting the correction $(A/B)^{D} - (A/B)^{H}$ from the measured rate $(A/B)^{D}$ one obtains the ratio $(A/B)^{H}$ which corresponds to pure H_2O. This value can be used directly to read out the value of k from Fig. 1 in the main text. For a specific ratio $(A/B)^{D}$ the correction depends on whether k is on the left (low k) or right side (high k) of Fig. 1.

where f is the fraction of deuterium in the solvent ($f = 0.03$ in our case, corresponding to 6% HDO). We have repeated the calculation of Fig. 1 in the main text, taking in to account the contribution of deuterium, starting with an initial density operator $\rho(0) = \{(1\text{-}f), 0, 0, 0, f, 0, 0\}$ and tracking the evolution of the total observable coherence $< N_y^{tot} > (t) =< N_y^{H} > (t) + < N_y^{D} > (t)$. Fig. A1 shows the difference between the ratios $(A/B)^{D} - (A/B)^{H}$ as a function of $(A/B)^{D}$ for different numbers of pulses n_{CPMG} in the sequence (the parameters used for the calculation were the same as in Fig. 1). The ratio $(A/B)^{H}$ refers to $f = 0$, while ratio $(A/B)^{D}$ corresponds to a partially deuterated solvent ($f > 0$). The largest difference between the ratios $(A/B)^{D} - (A/B)^{H}$ is about 0.012 for $f = 0.03$. We can now subtract this difference from $(A/B)^{D}$ to obtain the ratio $(A/B)^{H}$. This corrected value has been used in order to obtain k from Eqs. (A.1) and (A.2). One could also directly fit the results to the calculations which include deuterium, however, in practice, it was easier to fit k to the analytical expressions using the 4×4 matrix in Eq. (A.2). Since quadrupolar relaxation may be rapid, neglecting longitudinal auto-relaxation of deuterium may not be legitimate. However, inclusion of this rate, even if it is large, does not change the correction factor significantly.

References

[1] C.E. Dempsey, Hydrogen exchange in peptides and proteins using NMR spectroscopy, Prog. Nucl. Magn. Reson. Spectrosc. 39 (2001) 135–170.

[2] A. Wishnia, M. Saunders, The nature of the slowly exchanging protons of ribonuclease, J. Am. Chem. Soc. 84 (1962) 4235–4239.

[3] E. Grunwald, A. Loewenstein, S. Meiboom, Rates and mechanisms of protolysis of methylammonium ion in aqueous solution studied by proton magnetic resonance, J. Chem. Phys. 27 (1957) 630–640.

[4] S. Forsén, R.A. Hoffman, Study of moderately rapid chemical exchange reactions by means of nuclear magnetic double resonance, J. Chem. Phys. 39 (1963) 2892–2901.

[5] N.R. Skrynnikov, R.R. Ernst, Detection of intermolecular chemical exchange through decorrelation of two-spin order, J. Magn. Reson. 137 (1999) 276–280.

[6] C.T.W. Moonen, P. van Gelderen, G.W. Vuister, P.C.M. van Zijl, Gradient-enhanced exchange spectroscopy, J. Magn. Reson. 97 (1992) 419–425.

[7] A. Abragam, Principles of Nuclear Magnetism, Oxford University Press, 1961.

[8] F. Blomberg, W. Maurer, H. Rüterjans, ^{15}N Nuclear magnetic resonance investigations on amino acids, Proc. Natl. Acad. Sci. USA 73 (1976) 1409–1413.

[9] S. Meiboom, D. Gill, Modified spin-echo method for measuring nuclear relaxation times, Rev. Sci. Inst. 29 (1958) 688–691.

[10] S. Waelder, L. Lee, A.G. Redfield, Nuclear magnetic resonance studies of exchangeable protons. I. Fourier transform saturation-recovery and transfer of saturation of the tryptophan indole nitrogen proton, J. Am. Chem. Soc. 97 (1975) 2927–2928.

[11] P.R. Vasos, J.B. Hall, R. Kümmerle, D. Fushman, Measurement of ^{15}N relaxation in deuterated amide groups in proteins using direct nitrogen detection, in: Lecture at 47th ENC Conference, Asilomar, USA, 2006.

[12] A.J. Shaka, J. Keeler, T. Frenkiel, R. Freeman, An improved sequence for broad-band decoupling: WALTZ-16, J. Magn. Reson. 52 (1983) 335–338.

[13] R.S. Molday, S.W. Englander, R.G. Kallen, Primary structure effects on peptide group hydrogen exchange, Biochemistry 11 (1972) 150–158.